HHS Public Access

Author manuscript

Leukemia. Author manuscript; available in PMC 2022 November 01.

Published in final edited form as:

Leukemia. 2021 November ; 35(11): 3324–3328. doi:10.1038/s41375-021-01176-7.

Clonal trajectories and cellular dynamics of myeloid neoplasms with *SF3B1* mutations

Hassan Awada[1], **Cassandra M. Kerr**[1], **Arda Durmaz**[1], **Vera Adema**[1], **Carmelo Gurnari**[1], **Simona Pagliuca**[1], **Misam Zawit**[1], **Sunisa Kongkiatkamon**[1], **Heesun J. Rogers**[2], **Yogen Saunthararajah**[1,3], **Mikkael A. Sekeres**[3], **Hetty Carraway**[3], **Jaroslaw P. Maciejewski**[1,3], **Valeria Visconte**[1]

[1]Department of Translational Hematology and Oncology Research, Taussig Cancer Institute, Cleveland Clinic, Cleveland, OH, USA

[2]Department of Laboratory Medicine, Cleveland Clinic, Cleveland, OH, USA

[3]Leukemia Program, Department of Hematology and Medical Oncology, Taussig Cancer Institute, Cleveland Clinic, Cleveland, OH, USA

To the Editor:

Molecular lesions, either structural cytogenetic anomalies or gene mutations of known significance, occur in a step-wise fashion and are morphologic and prognostic markers in myeloid neoplasms (MNs). Current World Health Organization (WHO) classification categorizes patients with myelodysplastic syndrome (MDS) with ringed sideroblasts (RS) ≥15% or ≥5% RS with an *SF3B1* mutation (*SF3B1*^{MT}) as MDS-RS [1], a subtype in which the presence of *SF3B1* mutations confers a favorable prognosis [2–6]. Although most patients with *SF3B1*^{MT} have a classic phenotype, there is considerable heterogeneity within this subcategory including individual diversion of the originally favorable clinical phenotype. The disappearance of RS can be observed during the disease course of MNs, suggesting that new cellular shifts, due to the acquisition of additional lesions cooperating with/ or suppressing *SF3B1*^{MT} might go along with evolution to acute myeloid leukemia (AML). Such courses are likely a result of the type and configuration of *SF3B1*^{MT}, which potentially impact the disease course.

Valeria Visconte, visconv@ccf.org.

Author contributions Contribution: HA collected, analyzed and interpreted the data, designed the tables and figures, and wrote the manuscript; CMK, AD developed DNA-sequencing methodologies, analyzed single cell-DNA sequencing, and edited the manuscript; VA; CG, SP, MZ, SK, collected the data and edited the manuscript; HJR collected clinical info and provided critical review to the manuscript; YS, MAS, HEC provided patients and important insights to the manuscript preparation; JPM provided patients, laboratory space and facilities, granted a collection of clinical charts and molecular annotated databases, sponsored the DNA sequencing studies, and edited the manuscript; VV conceived the idea, designed the study, supervised the work, interpreted and analyzed the data and content, and wrote the manuscript.

Compliance with ethical standards

Supplementary information The online version contains supplementary material available at https://doi.org/10.1038/s41375-021-01176-7.

Conflict of interest The authors declare that they have no conflict of interest.

Inspired by a seminal work describing *SF3B1*^{MT} as a disease-defining molecular lesion in terms of survival and independent risk of clonal evolution [6], we looked closer at our preliminary observations suggesting that important biological clues can be extrapolated from the molecular associations of *SF3B1*^{MT} and their clonal architecture in the context of MNs [7]. To that end, we reviewed clinical and molecular annotations of patients with MNs with the intent of dissecting the *SF3B1* mutatome and describing whether the clonal rank (ancestral/dominant vs. sub-clonal/secondary) might alter the phenotypic cell trajectories. We identified 209 *SF3B1*^{MT} in about 6% of MN patients (209/3673). Clinical and molecular data of the cohort were collected at The Cleveland Clinic Foundation and retrieved from publicly available datasets (refer to Supplementary Material) for comparisons' purposes. The demographic, clinical and cytogenetic characteristics are summarized in Table S1. Using variant allele frequencies (VAFs) estimation that was previously confirmed by PyClone method [7, 8], *SF3B1*^{MT} were categorized as: (i) dominant (*SF3B1*^{DOM}, $n = 96$, 46%), (ii) secondary (*SF3B1*^{SEC}, $n = 68$, 33%) and as expected, due to the lack of resolution of the bioinformatics methods deployed, sub-categorization included transitional category of (iii) "co-dominant" (*SF3B1*^{COD}, $n = 45$, 21%). Schematic representations of these configurations are described in Fig. 1A. Despite the different hierarchical assignments with respect to other concurrent mutations, *SF3B1*^{MT} VAFs in the 3 groups did not statistically vary ($P = 0.07$; Fig. S1). In terms of survival, *SF3B1*^{COD} had a similar median OS to that of *SF3B1*^{SEC} (24.4 vs. 21.9 mo.) and a poorer outcome vs. *SF3B1*^{DOM} (41.1 mo.; $P = 0.03$; Fig. 1B). In terms of disease phenotypes, *SF3B1*^{COD} cases had no significant association with disease-type or cytogenetics vs. *SF3B1*^{DOM} and *SF3B1*^{SEC} (Table S2). The mutational profile of *SF3B1*^{COD} resembled that of *SF3B1*^{SEC}, while differences were found compared to *SF3B1*^{DOM} with a significant association with *ASXL1, DNMT3A, RUNX1 and TET2* mutations (Fig. S2A, B). Although some mutations (*DNMT3A*, 22%; *TET2*, 20%; *RUNX1*, 11%) were preferentially associated with *SF3B1*^{COD} (Fig. S3A), they had no prognostic power (Fig. S3B–D). Therefore, we focused on non-ambivalent hierarchical *SF3B1*^{MT} (mutations with >5% difference in VAFs; $\Delta VAF > 5\%$) as these showed higher degrees of distinction and a more stringent representation of the chronology of mutations defined as *SF3B1*^{DOM} vs. *SF3B1*^{SEC}.

As compared to *SF3B1*^{SEC}, *SF3B1*^{DOM} were enriched in MDS (33 vs. 18%; $P = 0.007$), particularly with RS (27 vs. 9%; $P = 0.006$) while less present in sAML (12 vs. 23%; $P = 0.03$) (Table S3, Fig. S4). Eighty-percent of *SF3B1*^{DOM} and 85% of *SF3B1*^{SEC} occurred in the elderly (age ≥ 60 years). No differences in sex distribution and hematological parameters were reported except for bi-cytopenia (52 vs. 36%; $P = 0.01$), more dysplastic myeloid cells (53 vs. 29%; $P = 0.01$) and bilineage dysplasia (47 vs. 26%; $P = 0.02$, Table S3) in patients with *SF3B1*^{SEC} vs. *SF3B1*^{DOM}. In contrast, the bone marrow of *SF3B1*^{DOM} patients was more often normocellular (46 vs. 29%; $P = 0.02$) and enriched with RS (Table S3); the latter also correlated with higher *SF3B1*^{MT} VAFs (Fig. 1C, Fig. S5). Interestingly, although patients with *SF3B1*^{SEC} had shorter OS than those with *SF3B1*^{DOM} (21.9 vs. 41.1 mo.; $P < 0.03$; Fig. 1B), when dichotomized according to different *SF3B1*^{MT} VAF ranges (>40%, 20–40%, <20%), no significant OS differences were observed (Fig. S6A) even when the *SF3B1*^{MT} clonal ranks were considered (Fig. S6B–D).

Therefore, we investigated the prognostic importance of distinct molecular associations in *SF3B1*^{DOM} and *SF3B1*^{SEC}.The analysis of the mutational burden showed that patients with *SF3B1*^{DOM} had fewer numbers of mutations per individual compared to those harboring *SF3B1*^{SEC} [1.0 (95/96) vs. 2.6 (179/68)]. The frequencies of mutations in *SF3B1*^{DOM} vs. *SF3B1*^{SEC} are depicted in Fig. 1D. In total, 274 concurrent somatic mutations were detected, of which 4% included co-hits in other RNA-splicing factor genes (*PRPF8, SRSF2, U2AF1, ZRSR2*; Fig. S7A, B and S8A–E) as recently described [9]; and of which 75% had a normal karyotype (Fig. S7C). Targeted deep sequencing of the most recurrently mutated genes in MNs revealed that concurrent myeloid mutations were more associated with *SF3B1*^{SEC} than *SF3B1*^{DOM}, suggesting that this increased accumulation of concomitant mutations might reflect a more pronounced susceptibility to clonal expansion. Indeed, univariate analyses showed significantly higher odds of mutations in *TET2* (41 vs. 11%; $P < 0.0001$), *RUNX1* (31 vs. 7%; $P < 0.0001$), *ASXL1* (18 vs. 2%; $P = 0.0005$), *BCOR*/*BCORL1* (15 vs. 5%; $P = 0.05$), *DNMT3A* (18 vs. 6%; $P = 0.02$) and *STAG2* (13 vs. 3%; $P = 0.01$) in individuals with *SF3B1*^{SEC} vs. *SF3B1*^{DOM} (Fig. 1E). We then applied multivariate analysis to confirm the independent relationships between *SF3B1* clonal status and other distinct genomic associations and found that *ASXL1, DNMT3A, IDH2, NF1, STAG2, TET2* and *RUNX1* significantly shaped the molecular profile of *SF3B1*^{SEC} (Fig. 1F). Moreover, mutations preceding *SF3B1*^{SEC} mainly affected lineage-restricted genes associated with repression of erythroid programs (*RUNX1*, 12%), cohesin complex (*STAG2*, 9%), transcriptional corepressors (*BCOR*/ *BCORL1*, 7%), terminal monocytic differentiation (*TET2*, 7%), chromatin remodeling (*ASXL1*, 6%) and leukemogenesis (*DNMT3A* and *FLT3*, 4% each) (Fig. S9). Thereby, we investigated whether specific concurrent mutations can impact the survival outcomes of *SF3B1*^{MT} MNs and further distinguish *SF3B1*^{DOM} vs. *SF3B1*^{SEC} subsets. Our analysis revealed markedly unfavorable outcomes in *SF3B1*^{SEC} compared to *SF3B1*^{DOM} when particular genes, e.g., *TET2*, co-existed (11.7 vs. 96.1 mo., $P = 0.01$; Fig. 1G) while the presence of *FLT3*^{MT} contributed to dismal prognosis only in *SF3B1*^{DOM} (8.4 vs. 47.6 mo., $P = 0.01$; Fig. 1H). The extent of prognostic variations between both *SF3B1*^{MT} configurations suggests that new lesions might represent key contributors to the distinct clinical course of *SF3B1*^{MT} MNs. The association between *TET2* and *SF3B1* mutations has been previously seen in MNs and in vivo functional studies described an exacerbated anemic phenotype when present [10]. The prognostic implication of *FLT3* mutation concurrence with *SF3B1* mutation might highlight a distinct subgroup of patients with more proliferative features.

Given the fact that inferring clonal architecture from bulk sequencing might not accurately describe that *SF3B1*^{MT} can exist in a secondary configuration and acquired during clonal evolution, we applied single-cell DNA sequencing to an MDS case with complex molecular architecture and dissected its clonal trajectory. We found a subclonal *SF3B1*^{MT} (p.K700E) to an ancestral *TET2*^{MT} (p.Y1618X), that coexisted in clones carrying *TET2* and *JAK2* (p.V617F) and *TET2*, *JAK2* and *TP53* (c.276+1G>A) (Fig. 1J). Additionally, to confidently assign the mutations we performed serial DNA sequencing on 21 patients' specimens to deeply define the clonal trajectories of *SF3B1*^{MT} in MNs. The study of the evolution of *SF3B1*^{MT} VAFs (Fig. 2A–J) demonstrated that a founder *SF3B1* clone (p.E622D) remained as such and increased in VAF (case #1, 2; the latter confirmed also by single-cell DNA

sequencing; Fig. 1I), became secondary due to acquisition of other hits (cases #3) or codominant (case #11). Of note, we found that in one case, *SF3B1*^{DOM} disappeared at the 2nd time point (case #4) possibly suggesting that the composition of the bone marrow at that time-point contained only a minimal fraction of cells carrying *SF3B1*^{MT}. In addition, *SF3B1*^{COD} clones remained co-dominant (cases #5, 6), became secondary (case #7) or dominant (case #8). The *SF3B1*^{SEC} clone remained secondary (case #12), disappeared (case #13, 16) or became dominant due to the disappearance of other founder mutations (case #14, 15). The clonal evolution elucidated by serial samples as well as bone marrow reviews, unveiled that an evolving AML phenotype was accompanied by the acquisition of novel lesions (*FLT3, PTPN11, RUNX1, TET2, WT1* in cases #17–19) or emerging cytogenetic abnormalities [inv(3) and del(5q) in cases #20, 21] driving transformation.

The mutational rank within clonal hierarchy is different from just assigning clonal burden and correlates with the outcomes of the mutations including *SF3B1*. Our study supports that specific disease phenotypes and clinical outcomes of patients with MNs are inferred by the clonal hierarchy of *SF3B1*^{MT}, not only its VAF%, with respect to other founder or subclonal myeloid events. This distinction allows for an even higher level of precision in predicting clinical outcomes of patients with *SF3B1* mutations. Both, methodological feasibility of VAF based clonal ranking and predictive value of *SF3B1* clonal hierarchy assessment in MN will need further confirmation. Additionally, we deciphered the clonal trajectories of *SF3B1*^{MT} and uncovered key events driving leukemic evolution in *SF3B1*^{MT} low-risk MDS. Hence, *SF3B1*^{MT} hierarchical configuration can potentially delineate the fate of *SF3B1*^{MT} MNs and further define this newly proposed disease-entity.

Supplementary Material

Refer to Web version on PubMed Central for supplementary material.

Acknowledgements

We thank the following sources of funding: Aplastic Anemia and MDS International Foundation Research Grant (VV and JPM), Vera and Joseph Dresner Foundation-MDS Research Fund (VV), VeloSano Pilot Award (VV), NIH/NHLBI R35HL135795 (JPM), R01HL132071 (JPM), The Henry and Marilyn Taub Foundation (JPM). We thank the team of Mission Bio for technical expertise on single cell-DNA sequencing and The Cancer Genome Atlas (TCGA), The BEAT AML Master Trial and The German-Austrian Study Group for data accessibility.

References

1. Arber DA, Orazi A, Hasserjian R, Thiele J, Borowitz MJ, Le Beau MM, et al. The 2016 revision to the World Health Organization classification of myeloid neoplasms and acute leukemia. Blood. 2016;127:2391–405. [PubMed: 27069254]
2. Yoshida K, Sanada M, Shiraishi Y, Nowak D, Nagata Y, Yamamoto R, et al. Frequent pathway mutations of splicing machinery in myelodysplasia. Nature. 2011;478:64–69. [PubMed: 21909114]
3. Papaemmanuil E, Cazzola M, Boultwood J, Malcovati L, Vyas P, Bowen D, et al. Somatic SF3B1 mutation in myelodysplasia with ring sideroblasts. N. Engl J Med. 2011;365:1384–95. [PubMed: 21995386]
4. Visconte V, Makishima H, Jankowska A, Szpurka H, Traina F, Jerez A, et al. SF3B1, a splicing factor is frequently mutated in refractory anemia with ring sideroblasts. Leukemia. 2012;26: 542–5. [PubMed: 21886174]

5. Malcovati L, Karimi M, Papaemmanuil E, Ambaglio I, Jädersten M, Jansson M, et al. SF3B1 mutation identifies a distinct subset of myelodysplastic syndrome with ring sideroblasts. Blood. 2015; 126:233–41. [PubMed: 25957392]

6. Malcovati L, Stevenson K, Papaemmanuil E, Neuberg D, Bejar R, Boultwood J, et al. SF3B1-mutant myelodysplastic syndrome as a distinct disease subtype - a Proposal of the International Working Group for the Prognosis of Myelodysplastic Syndromes (IWG-PM). Blood. 2020;136:157–70. [PubMed: 32347921]

7. Nagata Y, Makishima H, Kerr CM, Przychodzen BP, Aly M, Goyal A, et al. Invariant patterns of clonal succession determine specific clinical features of myelodysplastic syndromes. Nat Commun. 2019;10:5386. [PubMed: 31772163]

8. Awada H, Nagata Y, Goyal A, Asad MF, Patel B, Hirsch CM, et al. Invariant phenotype and molecular association of biallelic TET2 mutant myeloid neoplasia. Blood Adv. 2019;3:339–49. [PubMed: 30709865]

9. Taylor J, Mi X, North K, Binder M, Penson A, Lasho T, et al. Single-cell genomics reveals the genetic and molecular bases for escape from mutational epistasis in myeloid neoplasms. Blood. 2020;136:1477–86. [PubMed: 32640014]

10. Obeng E, Chappell R, Seiler M, Chen MC, Campagna DR, Schmidt PJ, et al. Physiologic expression of Sf3b1(K700E) causes impaired erythropoiesis, aberrant splicing, and sensitivity to therapeutic spliceosome modulation. Cancer Cell. 2016;30: 404–17. [PubMed: 27622333]

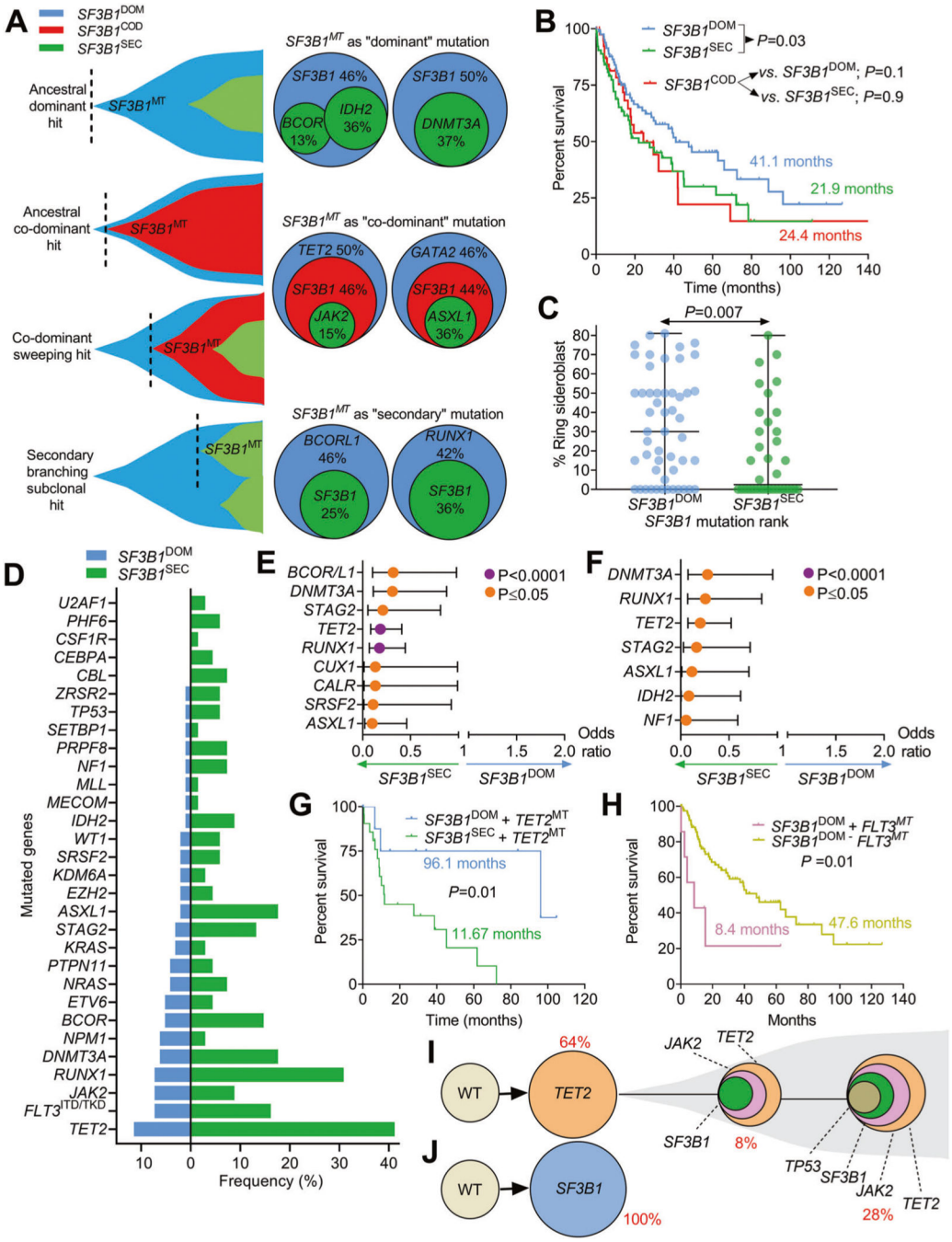

Fig. 1. Characteristics, mutational associations and prognostic implications of clonal events in *SF3B1* mutant myeloid neoplasms.

A Fish plots and pie charts depicting different examples of *SF3B1* mutations clonal status and its secondary mutations in the case of *SF3B1* dominant (*SF3B1*^{DOM}), *SF3B1* co-dominant (*SF3B1*^{COD}) and *SF3B1* secondary mutations (*SF3B1*^{SEC}). **B** Kaplan–Meier curves showing the overall survival of cases with *SF3B1* mutations per clonal status (dominant, secondary, co-dominant). The curves represent the percent survival of patients with dominant, co-dominant and secondary *SF3B1* mutations. Comparisons of survival

in dominant versus secondary *SF3B1* and co-dominant versus dominant and secondary were done. Levels of statistical significance was calculated by *P* values. **C** Scatter plot describing the percentage of ringed sideroblasts in patients with *SF3B1* dominant (blue) vs. secondary (green) mutations. Levels of statistical significance was assessed by *P* values using Mann–Whitney U test. **D** Bar graph showing the frequency (in percentage) of a panel of myeloid gene mutations co-occurring with *SF3B1* mutations in dominant vs. secondary status. **E** Univariate analysis showing the odds ratio representing the strength of the association of *SF3B1* mutations with other gene mutations. Levels of statistical significance is indicated in purple and orange colors ($P < 0.0001$ and $P \leq 0.05$) using Fisher's Exact test. **F** Multivariate analysis showing the odds ratio representing the strength of the association of *SF3B1* mutations with other gene mutations. Levels of statistical significance is indicated in purple and orange colors ($P < 0.0001$ and $P \leq 0.05$) using Fisher's Exact test. **G** Kaplan–Meier curves showing the impact of *TET2* mutations (*TET2*^{MT}) on *SF3B1* mutant cases per hierarchical *SF3B1* mutational configuration: *SF3B1* dominant (*SF3B1*^{DOM}) vs. secondary (*SF3B1*^{SEC}). Levels of statistical significance was calculated by *P* values. **H** Kaplan–Meier curves showing the impact of the presence of *FLT3* mutations (*FLT3*^{MT}) on *SF3B1* dominant (*SF3B1*^{DOM}) cases. Levels of statistical significance was calculated by *P* values. Single cell-DNA sequencing revealing the clonal trajectories of one sample with (**J**) ancestral/founder *SF3B1* mutation and another sample with secondary/subclonal *SF3B1* mutation (**I**). Different colors represent different mutations.

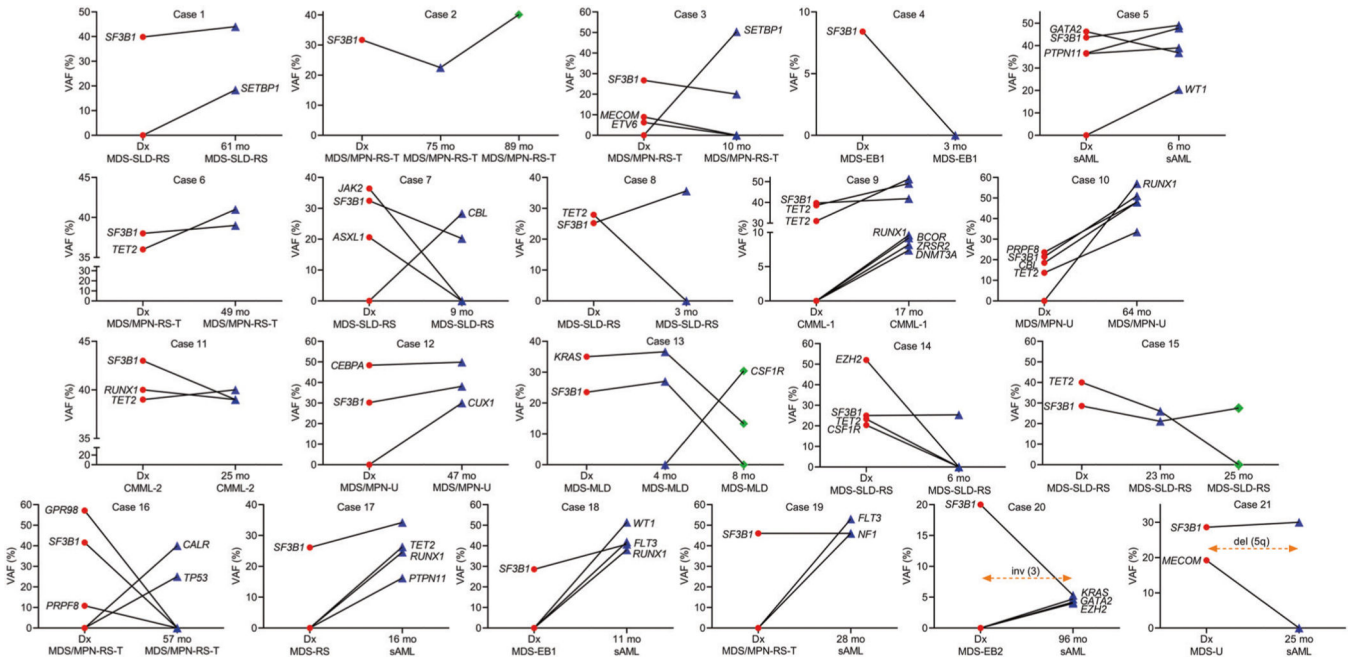

Fig. 2. The clonal trajectories of *SF3B1* mutations.

Serial analysis of patients with myeloid neoplasia and *SF3B1* mutations. DNA specimens from 21 samples with *SF3B1* mutations were analyzed at 2 or 3 time points. Targeted sequencing panel for myeloid genes was applied to all samples. Line graphs indicate variant allele frequency in percentage for mutations considered somatic. Red, blue and green colors indicate mutations at first time point, second and third time point, respectively. Dx diagnosis, VAF variant allele frequency, mo months.